Fractals in Monte Carlo simulations of a short polyelectrolyte

1999 J. Phys. A: Math. Gen. 32 235

(http://iopscience.iop.org/0305-4470/32/2/002)

J. Phys. A: Math. Gen. **32** (1999) 235–248. Printed in the UK PII: S0305-4470(99)96043-2

Fractals in Monte Carlo simulations of a short polyelectrolyte

Chava Brender†, Meir Danino and Smadar Shatz
Department of Physics, Bar-Ilan University, Ramat-Gan 52900, Israel

Received 17 July 1998, in final form 16 September 1998

Abstract. Fractal dimensionalities, d_f, for charged polymers are calculated over a continuous range of Bjerrum length λ for chains with various numbers of beads, N. Drastically decreasing values of d_f, characteristic of a phase transition, are found as λ increases from zero in the range $0 < \lambda < 1$ Å. The fractal dimensionality approaches unity as predicted by de Gennes *et al* (de Gennes P-G, Pincus P, Valesco R M and Brochard F 1976 *J. Physique* **37** 1461) close to the onset of order. A newly developed smoothing algorithm yields a substantial improvement in the MC results and reveals an interesting fan-shaped behaviour of exponents and prefactor components at λ slightly above zero. It also enables discernment of a non-monotonic behaviour of d_f versus N at $\lambda = 0$ and close to zero. Differences found in bending between short and long chains may provide an additional explanation for the stability of benzene and the low stability of conjugated rings of $N > 6$. Based on fractal concepts, monomer densities are derived at various λ and it is suggested that the drastic density changes at $0 < \lambda < 1$ Å are evidence of the first-order nature of this phase transition.

1. Introduction

Since the concept of scaling was first introduced to the field of polymers [1], exponent determination has become one of the main goals in polymer investigations. In short polyelectrolyte chains, it was found that there is difficulty in calculating the exponents by means of the usual log–log plots of the radius of gyration or end-to-end distance versus N. Using this usual method (denoted as method I_a) the slopes obtained for polyelectrolytes at various λ *become higher than* 2 above $\lambda = 0.5$ Å for $\langle S^2 \rangle$ and above 1.5 Å for $\langle R^2 \rangle$. The Bjerrum length λ is defined as z^2e^2/DkT, where z is the charge on each ion of the chain and D is the dielectric constant of the solvent. Because a chain cannot be more than fully extended, these results have no physical meaning. For a detailed explanation see [2]. Slopes higher than 2 were also reported in [3]. In [4] different slopes were obtained when N was varied. In this paper we attempt to overcome this difficulty by the calculation of exponents from a different viewpoint using the fractal concept. For the first time, to the best of our knowledge, the *fractal dimensionality*, d_f, of a polyelectrolyte is calculated *over a continuous range of* λ, using the method developed in [5–10] for self-avoiding walk (SAW) chains (denoted as method II). In this paper we describe how the exponents are varied as functions of both high and low λ. At high λ we describe the exponents for bare polyelectrolyte chains and for polyelectrolyte with added salt. At low λ, the Monte Carlo (MC) results display noise. To decrease the noise component, we have developed a smoothing technique described in this article. Modelling and simulation techniques are described in the next section. Fractal parameters are introduced

† E-mail address: brender@mail.blu.ac.il

0305-4470/99/020235+14$19.50

in section 3. The results and smoothing technique are discussed in section 4 followed by summary and concluding remarks in section 5.

2. Model and simulation technique

The fully charged chain, represented by N hard spherical beads on a lattice, was discussed in detail in previous papers [11, 12]. The charge is equally distributed on a chain of N beads of diameter $b = 4$ Å located in a cubic box. The box has a length of 2048 Å and satisfies periodic boundary conditions. An initial configuration of a polyion is chosen and the system is permitted to relax toward an equilibrium configuration by successive random motions of the beads. The relaxation technique of the polymer is a dynamic MC scheme, involving simple flips together with complicated crankshaft motions. After each cycle or a trial move (bead dynamics is discussed in [13]), the electrostatic energy of the system is computed using the minimum image approximation described in [13] and in the references therein. According to Metropolis [14] one decides to accept or to reject the new configuration. The slow annealing Kirkpatrick procedure [15] is used for the whole range of λ. We decrease the temperature in stages using the last accepted conformation from the previous temperature as a starting conformation for the succeeding stage in the annealing procedure until we reach a low temperature. Two cases are considered, the bare chain having no added salt ($C = 0$ M) and the Debye–Hückel (DH) screened chain with added salt ($C \neq 0$ M), where the Coulombic potential is replaced by the screened Debye–Hückel potential assuming a uniform distribution of point ions near the polyion. Calculations were done for $N = 8$, 16, 32, 48, 64, 70 and 80 (at $\lambda > 0.5$ Å). MC simulations were carried out on IBM 3090, RS/6000 and SP/2 computers at Bar-Ilan University for chain lengths between 8 and 80 beads at various values of an independent parameter λ [11], the Bjerrum length, defined as z^2e^2/DkT, where z is the charge on each ion of the chain and D is the dielectric constant of the solvent. At room temperature for a polyelectrolyte in water solution, $\lambda = 7.14$ Å. The variation of λ, can be done by varying each of the parameters: temperature, bead charge (partial charging or counter-ions screening [16]) and dielectric constant [11]. For simplicity, λ can be thought of as a reduced inverse temperature. In [16], the polyelectrolytes expansion was generalized to also represent neutral polymer expansion, thus the λ scale can be viewed also as an expansion parameter for the chain unfolding process. Ensemble averages were collected after rejecting the initial cycles before relaxation. Subsequent groups of 10 000 cycles were averaged separately and averages of the means over all groups were then calculated. A total number of 3 600 000 cycles was generated for each run. To achieve equilibrium results for the d_f parameters in the vicinity of $\lambda = 0$, 40 independent runs each of 10 000 000 cycles were performed for N between 8 and 80 beads at $\lambda = 0$. For λ close to zero, 10 such independent runs were performed. Because of noise in the values of d_f and in the values of B (see equation (4)) at low λ, we investigated additional values of N at smaller intervals for $\lambda \leqslant 0.5$ Å.

In this study, an exact zero value was substituted for λ rather than $\lambda = 10^{-4}$ Å as used in our previous studies. The use of the exact zero value is especially significant for the parameters which display sharp drops in the vicinity of $\lambda = 0$.

3. Fractal dimensionality from internal distances (method II)

Following the concept of polymer scaling introduced by de Gennes [17], and the fractal ideas presented by Mandelbrot [18], a *fractal dimensionality* of a polymer, d_f, was presented [6] using *internal distances* in the chain. Based on renormalization group theory arguments, it

was shown in [6] that for neutral polymers, d_f is related to the end-to-end exponent ν by:

$$\nu = 1/d_f. \tag{1}$$

Then, by analogy to the mean square end-to-end distance,

$$\langle r_n^2 \rangle \propto n^{2\nu} \propto n^{2/d_f} \tag{2}$$

where $\langle r_n^2 \rangle$ is the mean square distance of all subchains of n links in a chain of N beads averaged over the whole polymer chain. Thus,

$$\langle r_n^2 \rangle^{\frac{1}{2}d_f} \propto n. \tag{3}$$

Therefore,

$$\ln n = d_f \ln \langle r_n^2 \rangle^{\frac{1}{2}} + B. \tag{4}$$

According to equation (4), a plot of $\ln n$ as a function of $\ln \langle r_n^2 \rangle^{1/2}$ is linear with slope d_f and intercept B. The $\langle r_n^2 \rangle$ values are the averages of r_n^2, collected in a vector array $D(n)$ [16]. The collection and averaging are done as described for the other parameters (see section 2). Following [6], the mean square distances we use to determine d_f according to equation (4) are only those distances included in the 'main range', $(N/4 < n \leqslant 3N/4)$. In other words, for the d_f calculation, half of the members of the $D(n)$ vector array are discarded, those of very small n and very large n.

Averages are taken over millions of chains with the same number of beads as is normally done in dynamic MC calculations. The described method was found to be useful for fractal dimensionality derivation for neutral chains [5–10]. Owing to the self-similar character typical of any polymer, we anticipated that this method would also work in the case of charged macrochains. The description below supports this anticipation. An introduction to fractal geometry is presented in [19, 20]. Several recent papers concerning three-dimensional SAW chain investigations are referenced in [21–30]. An interesting review on the development of renormalization group concepts is presented in [31].

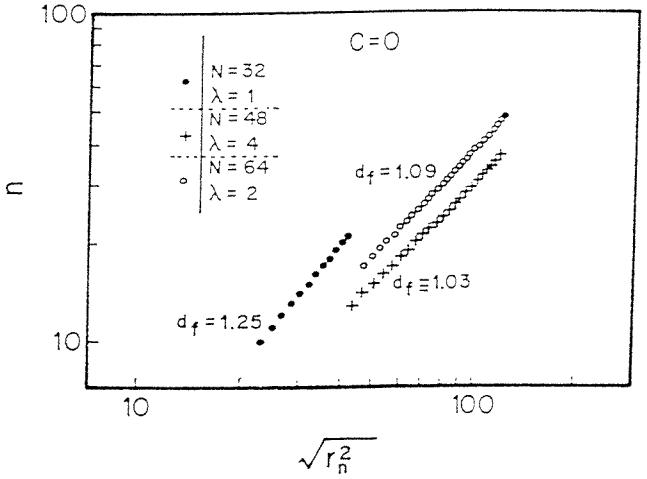

Figure 1. Plots of $\ln n$ versus $\ln \langle r_n^2 \rangle^{1/2}$ for three examples of bare polyelectrolyte chains with various N and λ (Å). The line slopes are the fractal dimensionalities (see equation (4)).

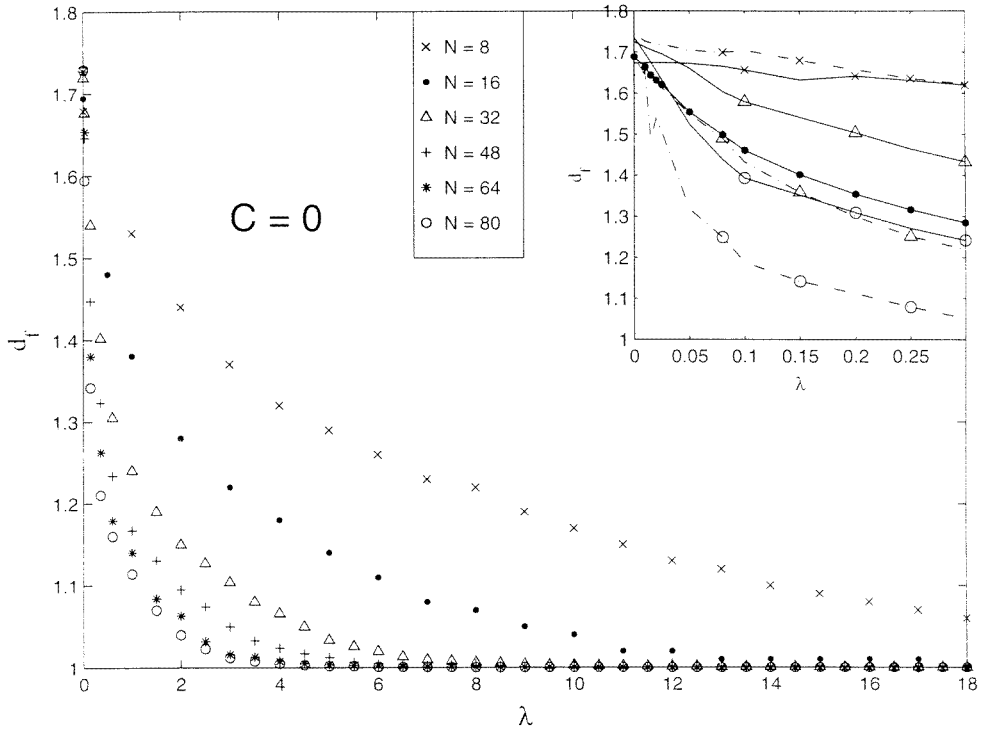

Figure 2. Raw data of fractal dimensionality d_f versus λ (Å) at various N for a bare polyelectrolyte chain ($C = 0$). Estimated errors are the standard deviations of the line intercepts. For the raw data, error bars are not shown because they are shorter than the markers. The inset shows plots of d_f for $N = 8$, 32 and 80 on an expanded scale of λ (Å) shown by full curves (calculated by method II). Plots of $2/[\mathrm{d}\ln\langle S^2\rangle/\mathrm{d}\ln N]$ (i.e. $2/2\nu_s$) for $N = 8$, 32 and 80 (dot-dash curves) are calculated by method I_b, i.e. numerical differentiation of $\ln\langle S^2\rangle$ with respect to $\ln N$. Markers are added to associate each curve with the corresponding N. Exponent values calculated by method I_a (see section 4.1.2) are plotted by a curve with solid dots.

4. Results and discussion

4.1. Bare polyelectrolyte ($C = 0$)

4.1.1. Calculation of d_f from internal distances. In figure 1, values of $\ln n$ are plotted versus $\ln\langle r_n^2\rangle^{1/2}$ for several N and λ. As anticipated, straight lines of high correlation (0.9998–1.0000) were obtained in all the investigated cases. Three typical examples of such best-fit lines are shown in figure 1. As seen from equation (4), the slopes of the straight lines are the chain fractal dimensionality d_f. The values of d_f for various N, derived as described above, are plotted against λ in figure 2. The estimated errors in d_f, i.e. the standard deviations of the slopes of the lines (depicted in figure 1), are smaller than the size of the symbols used in the plots (except for $\lambda = 0$, see figure 4 and explanation at the end of section 4.1.2 and in [32]). To check the validity of obtained results of d_f and B we use them to calculate $\langle S^2\rangle$ (according to equations (5) and (6)) and compare with the $\langle S^2\rangle$ values calculated directly from the simulations by an independent method. d_f and B can be related to $\langle S^2\rangle$ through equation (12) of [33]:

$$\langle S^2\rangle = \frac{1}{N^2}\sum_{i=1}^{N-1}\sum_{j=i+1}^{N}\langle r_{ij}^2\rangle \tag{5}$$

where $\langle r_{ij}^2 \rangle$ is the same as $\langle r_n^2 \rangle$ (see equation (4)). Rearranging equation (4), we get

$$\langle r_{ij}^2 \rangle = \mathrm{e}^{-2B/d_\mathrm{f}} |i - j|^{2/d_\mathrm{f}} \tag{6}$$

where $n = |i - j|$. To calculate $\langle r_{ij}^2 \rangle$ we substitute in (6) the values of d_f and B obtained from the polyelectrolyte simulations at various λ and N. We then substitute the $\langle r_{ij}^2 \rangle$ values into equation (5) to calculate $\langle S^2 \rangle$. Over the entire range of the investigated λ, the $\langle S^2 \rangle$ values obtained agree within one per cent with the values of $\langle S^2 \rangle$ that we obtained from simulations for $32 \leqslant N \leqslant 80$. For $N = 8$ and $N = 16$ the values agree within two per cent. This agreement confirms the validity of the d_f, B and $\langle S^2 \rangle$ of the MC results for the whole range of the investigated N.

4.1.2. d_f values at various λ. Havlin and Ben-Avraham [9] found a constant d_f value of 1.68 for an ensemble of SAW chains generated by the enrichment technique [34]. We find an increase in d_f from 1.68 to 1.75 as N increases from eight up to $N \leqslant 70$. It appears that this behaviour is non-monotonic (see section 4.3.1). Above $N = 70$, the d_f values decrease. Calculations for NSAW chains in [2] yields a value of $d_\mathrm{f} = 1.66$ for $N \to \infty$. This value agrees with the $\frac{5}{3}$ value obtained from Flory's exponent [35].

As λ increases, the chain expands because of electrostatic repulsion. This causes an increase in the exponent of n in equation (2) which means that ν increases and its reciprocal d_f, decreases. Figure 2 shows the decrease of d_f during the chain expansion from coil to rod at all N. As λ increases, the values of the markers for small N decrease while separating widely. The markers for $N \geqslant 48$, however, almost coincide. This indicates that there are large size effects for chains of $N < 48$, and that the exponent d_f is not independent of N as assumed by equation (2). All d_f results obtained by method II are equal or greater than unity and do not display the physically impossible results for exponents obtained by the usual log–log method.

The steepest drop in values of d_f is found between $\lambda = 0$ and $\lambda = 1$ Å for all investigated N. These drastic changes, characteristic of a phase transition, are caused by conformational variations. The sharp decrease in d_f between $\lambda = 0$ and $\lambda = 1$ Å in figure 2 for $N \geqslant 32$ is similar to the sharp decrease in the average number of contacts shown in figures 14 and 15 of [12]. It might be that the changes in the average number of contacts in a polymer chain cause a drastic change in its fractal dimensionality. Alternatively, there might be a phenomenon caused by configurational factors that has not yet been investigated. Note that these sharp changes in the values of d_f occur at low λ, far from $\lambda \sim 8$ Å, the range in which Brender found that the mean straight length $\langle l_s \rangle$ exhibits another transition [36].

In figure 2 it is seen that the value of λ, at which d_f approaches the theoretical value of unity predicted by de Gennes *et al* [37] is lower for larger values of N. For $N = 80$ this occurs near $\lambda = 2$. We expect that for $N \to \infty$ the theoretical d_f value will be obtained at lower λ.

The inset in figure 2 shows smoothed data of d_f for various N for $\lambda \leqslant 0.3$ Å (full curves) together with dot-dash plots of $2/[\mathrm{d} \ln\langle S^2 \rangle / \mathrm{d} \ln N]$ (i.e. $2/(2\nu_\mathrm{s})$ where the subscript s denotes radius of gyration). The latter values are calculated by numerical differentiation (using cubic spline approximation) of the MC $\ln\langle S^2 \rangle$ values with respect to $\ln N$. The inset shows clearly that, similar to d_f, $1/\nu_\mathrm{s}$ depends on N. This similarity in the behaviour of the various exponents supports the validity of method II. We designate the above method of exponent calculation, i.e. the differentiation of $\ln\langle S^2 \rangle$, as method $\mathrm{I_b}$ to distinguish it from method $\mathrm{I_a}$, which also uses $\langle S^2 \rangle$ values, but as log–log lines versus N. The usual log–log method, $\mathrm{I_a}$ yields the curve with solid dots shown between the dot-dash derivative curves. The location of this curve between the derivative curves, demonstrates that the usual method, $\mathrm{I_a}$ yields exponents for a chain whose length is the *mean* of the investigated chain lengths rather than for an infinite chain as

would be expected. This occurs because the slope of the $\ln\langle S^2\rangle$ versus $\ln N$ curve varies very slowly, i.e. d_f varies slightly with N. Within the limited range of N values, this variation is not easily seen but it is revealed by numerical differentiation locally with respect to $\ln N$. Despite this, performing linear regression on these data would yield, with a high correlation, a slope parameter which is the *mean* of the slope values of the curve, and not the slope of an infinite chain.

The mean square end-to-end exponent calculations from simulations of long chains performed by Higgs and Orland [38] supply additional confirmation to our results for $d_f = 1$ at low λ.

The fractal dimensionality may also be used as a measure of the curvature of the chain. In a rod-like configuration, $\langle R_N^2\rangle$ is proportional to N^2, i.e. $\nu = 1$. This implies, according to equation (1), that $d_f = 1$. Configurations that are more coiled have values of $d_f > 1$. It is apparent in figure 2, that, at $\lambda > 0$, the most coiled configuration over the investigated N is at $N = 8$. In other words, for $\lambda > 0$, the highest values of d_f over the range of investigated N are for $N = 8$. Figure 2 resembles figure 8 of [39] in that the highest values are for $N = 8$ with values decreasing at higher N in the same order. The different behaviour of d_f curves for chains with low N emphasizes the size effects found previously in this charged polymer system [16, 39].

The differences found in the chain curvatures d_f and the kink fraction, g [39], for various values of N under the same physical conditions may imply, from a chemical point of view, that reactivity of polyions varies with chain length. A reactant may find it easier to attack a long chain rather than a short one because the longer chain is more likely to be rod-like and have less steric hindrance. Aggregation of rod-like chains may be easier than that of bent chains. If so, the aggregation of long charged chains is expected to be more probable than that of short ones. The same ease of approach to a long chain may apply also to ion condensation and, in addition, may be a cause for a screening size effect [40]. The differences in bending between short and long chains may be an additional cause for the preference for cyclization found in short electron-rich chains. These differences in bending may provide an additional explanation for the stable structure of benzene consisting of $N = 6$ carbon atoms [42]. They might also explain the low probability for the existence of conjugated rings at N higher than six where the polymer chain's strong tendency to straighten itself reduces the stability of the cyclic structures.

Differences in chain curvature may also influence the packing structure of a system of several polyions [43]. It would be interesting to investigate whether such differences in curvature (at low λ) also contribute to N-dependent mobility (at low electric field) in the gel electrophoresis of DNA [44].

As an aside, it is seen in figure 4 that the largest fluctuations in d_f at all values of N are found at $\lambda = 0$. Fluctuations are a characteristic of phase transitions as, for example, in superconductivity [45]. The reason may be that, near $\lambda = 0$, there are the greatest number of configurations with the largest variety of shapes. In fact, at $\lambda = 0$, contacts, which are closed configurations, exist together with open configurations. As λ increases, the closed contacts are the first to disappear [12]. Note, however, that the maximum deviations in $\langle S^2\rangle$ and $\langle R^2\rangle$ are not at $\lambda = 0$ but at $\lambda = 4$ Å for $N = 32$ [11] and at $\lambda = 2$ Å for $N = 80$.

It is interesting to note that, from figure 2, we see that, as a polyelectrolyte chain unfolds, there is a rapid rise in $\nu(\nu = 1/d_f)$ followed by a levelling off at $\nu = 1$. This differs from the results in table VI of [46], table VII of [47] and table II of [48] where, for a polymer varying from a three-dimensional SAW to a two-dimensional SAW, a trough was found between $\nu = 0.6$ and $\nu = 0.75$. The difference in exponent behaviour points out, as is to be expected, that the mechanism of the chain variation is different in the two cases.

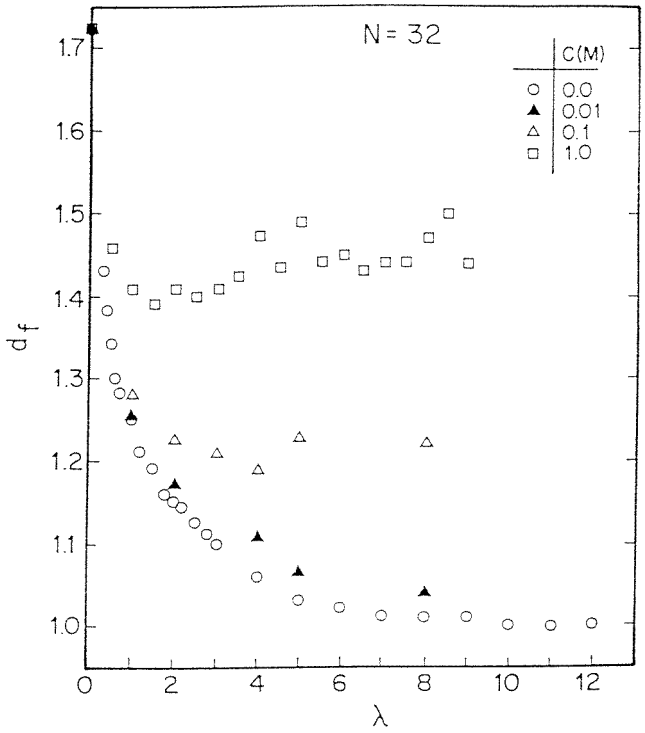

Figure 3. Values of d_f versus λ (Å), for a polyelectrolyte chain of $N = 32$ beads in various salt concentrations C (mol l^{-1}).

4.2. Polyelectrolyte with added salt ($C \neq 0$)

At this stage of the investigation, we use the Debye–Hückel screening potential as a simple qualitative method to introduce salt into the polyelectrolyte complex system. This research tool enables us to obtain a detailed picture of the shape of the charged chains by a method less time-consuming than that described in [13, 49].

At $C \neq 0$, exponents are obtained, to the best of our knowledge for the first time, over a continuous range of λ. According to equation (4), d_f is calculated from internal distances, with correlation values usually close to unity. Values of d_f versus λ, for various salt concentrations are shown in figure 3. We observe a tendency for d_f to increase as the salt concentration increases. For $C \leqslant 0.01$ M, the d_f values are close to those for $C = 0$. Only for $C = 0.1$ M and $C = 1$ M, are the d_f values significantly higher than the values for $C = 0$ at $\lambda > 0$. This is caused, at each λ, by the chain becoming more coiled with increased salt screening. The sensitivity of d_f to salt concentration is reminiscent of the mid-range sensitivity to salt concentration shown by the average number of kinks and by $\langle S^2 \rangle$ [11, 39]. It does not resemble the low sensitivity to salt of the average number of contacts $\langle n_t \rangle$ (figure 14 in [12]). This may indicate that d_f is influenced by bonds that are stronger than the contacts, i.e. bonds that do not open at low λ [12]. Note that for $C = 1$ M and $N = 32$, values of $\langle S^2 \rangle$ are close to the values for SAW chains (figure 1 in [11]), while the values of d_f are much lower than their SAW value.

Note also that with a salt concentration of only 0.1 M in the vicinity of the polymer or approximately 10^{-2} M in the bulk [49], the chain is no longer rod-like even at $\lambda > 6$ Å. For single polymer chains of $N > 32$, this concentration may be much lower [49]. Polyelectrolytes with even very low counter-ion concentrations, therefore, may have a tendency to avoid the

rod-like structure. In table 2 of [40], polyelectrolytes of $C = 1$ M at certain values of λ were shown to be equivalent to polyelectrolytes of $C = 0$ at lower λ. In other words, *addition of salt to polyelectrolyte solutions is equivalent to heating them*. Thus, the strong fluctuations of d_f found in the region of $C = 1$ M may be similar to the strong fluctuations found in the vicinity of $\lambda = 0$ (see section 4.1.2 above and section 4.4 below). This requires further investigation.

As physical conditions change between $\lambda = 0$ and $\lambda = 1$ Å, a sharp decrease in d_f occurs at both $C = 0$ (see figure 2 above) and $C \neq 0$ (even at $C = 6$ M, not shown). It can be observed from figure 3 that this decrease is greatest at lower C. It also can be observed from the figure that for $C = 0.1$ M, $N = 32$, d_f levels off at approximately 1.2. For $N = 32$, $C = 1$ M, it levels off at 1.45 and for $C = 2$ M, it levels off close to 1.56 (not shown). Further study is required to determine the behaviour of $C \neq 0$ for various other values of N.

Over the entire range of $\lambda > 0$, large chains have higher repulsion because of the long-range Coulomb interaction (each added bead is charged). Therefore their d_f decreases more sharply, as can be seen from figure 2. Adding salt to the charged chains reduces the repulsion due to the screening, which changes the interaction to a finite-range one. This causes the screened polyelectrolyte chain to almost recover the SAW chain structure, as can be seen from figure 3 and from figure 1 in [11]. We expect this recovery to be sharper at higher N.

In [50, 51] Wright *et al* examined various proteins bound to a DNA molecule (highly charged polyelectrolytes). Brender suggested [52] that the proteins do not have the same effect on the bending of the DNA because the different proteins have different charge distributions. As shown in figure 3, d_f is sharply dependent on salt concentration and is also extremely sensitive to λ which is charge dependent (see section 2). Just as salt screens the charge on the polyion and induces structural changes in the chain, so too does the protein which surrounds the DNA (section III.E in [40]). Proteins which have different charge densities, are expected, therefore, to screen differently.

4.3. Polyelectrolyte near $\lambda = 0$ (NSAW)

4.3.1. d_f versus N at low λ—the fan-shape. We now discuss the SAW chains that correspond to polyelectrolyte systems with $\lambda = 0$. To determine the behaviour of the exponent d_f as a function of N at $\lambda = 0$, we examine its values in the *vicinity* of $\lambda = 0$ and denote these chains as NSAW chains, *nearly self-avoiding walk* chains. The MC results for d_f and $-B$ in the range of $0 < \lambda \leqslant 0.5$ Å display much more noise than the results found for higher values of λ. Possible reasons for this high noise are discussed in section 4.1.2, above. To reduce the noise, we developed a smoothing technique described in section 4.4 below. The improved MC results, still exhibiting some noise, are shown in figure 4 where it can be seen that, for $\lambda = 0$, d_f rises as N increases except for a slight decrease at $N = 80$. From the results for $\lambda = 0$ alone, it is difficult to draw a conclusion as to the behaviour of d_f at higher N. The single drop recorded might possibly be nothing more than residual noise. Yet, the curves for λ slightly above zero show an increase of d_f with N up to a maximum value at N_{max} followed by slowly decreasing values. It is clearly seen that *the value of N_{max} increases as λ decreases toward zero*. The behaviour of d_f at λ close to zero and $N \leqslant 80$ might be an indication that, for $\lambda = 0$, there is also a slow decrease in d_f at high N with N_{max} in the vicinity of $N = 80$. It is possible, however, that, at $\lambda = 0$, the behaviour is different and that the value of d_f approaches a constant or perhaps continues to increase. A non-monotonic behaviour for SAW chains was also obtained in a study of correction-to-scaling of linear polymers in three dimensions [41]. Differing from the single value of 1.68 for all N found by Havlin and Ben-Avraham [9], our results, using the same 'main range' (see section 3) based on an MC method and present-day facilities, reveal a variation of d_f with N. Note that, in the range of $N \leqslant 70$ at $\lambda = 0$, the

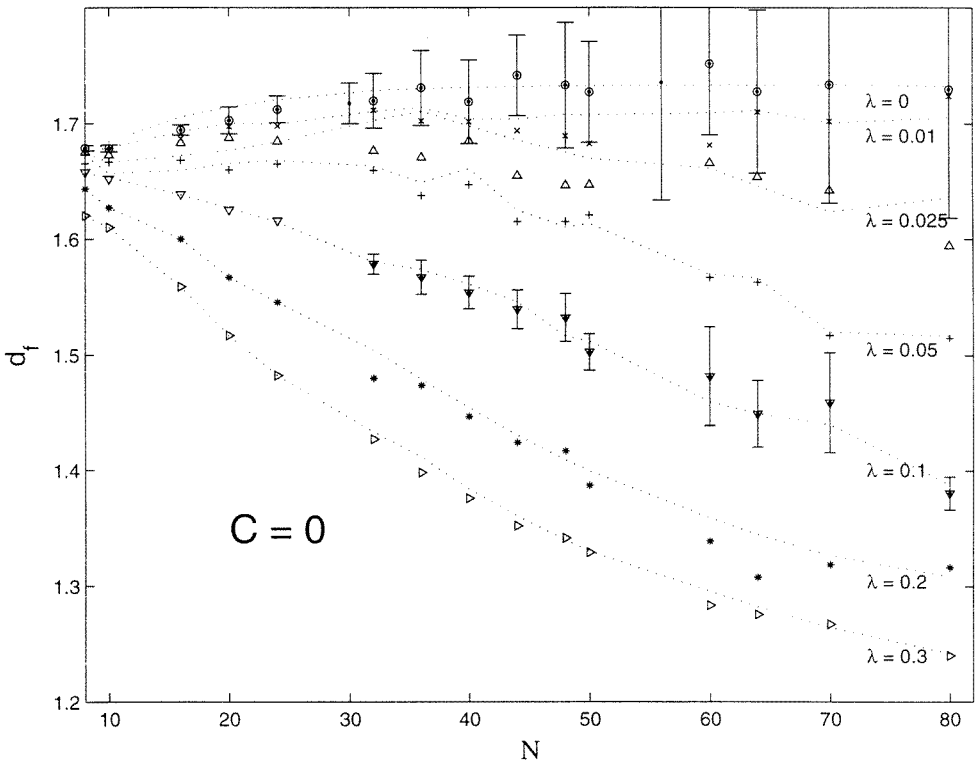

Figure 4. Fractal dimensionality d_f versus N for a polyelectrolyte chain at $\lambda = 0$ (SAW) and at λ (Å) values in the close vicinity of $\lambda = 0$ (NSAW). The markers display the raw data. The dotted curves display the smoothed data (see section 4.4). Error bars of raw data for $\lambda = 0$ and for $\lambda = 0.1$ Å are shown for various N. These are longer for higher N (see [30]). As λ increases from zero, error bars are shorter as shown for $\lambda = 0.1$ Å. Curves are connected to guide the eye.

longer the chain, the higher the values of d_f (and, as seen from figure 4, the estimated errors as well [32]). At $\lambda = 0.1$ Å, this trend for d_f has already reversed. The reversal occurs, therefore, between $0 < \lambda < 0.1$ Å where both increase and decrease of d_f versus N are seen at each λ. The transition between the two regimes is seen by the intersection of curves of d_f versus λ for the various values of N. In the inset of figure 2 this is seen for the range of $0.02 < \lambda < 0.04$ Å. Similar behaviour is found (not shown) for the intercept parameter B (defined in equation (4)).

4.3.2. Values of $-B$ versus N at low λ—the fan-shape. Figure 5 shows values of $-B$ (defined in equation (4)) versus N for various λ in the vicinity of $\lambda = 0$ (NSAW). In the following section we discuss the need for smoothing the data and explain the smoothing technique we developed. The raw data (discrete markers), and the smoothed data (dotted curves) are shown in figure 5. The salient feature of this graph is its resemblance to the fan-shaped graph obtained for d_f (figure 4). For long chains at $\lambda = 0$, the raw data does not display a clear monotonic trend with respect to N (similar to the case of d_f in section 4.3.1 above).

4.4. Smoothing technique

The results from simulations for d_f and $-B$ in the close vicinity of $\lambda = 0$ ($0 < \lambda < 0.5$ Å) display much more noise than is found at $\lambda > 1$ Å. To lower the noise component, we developed

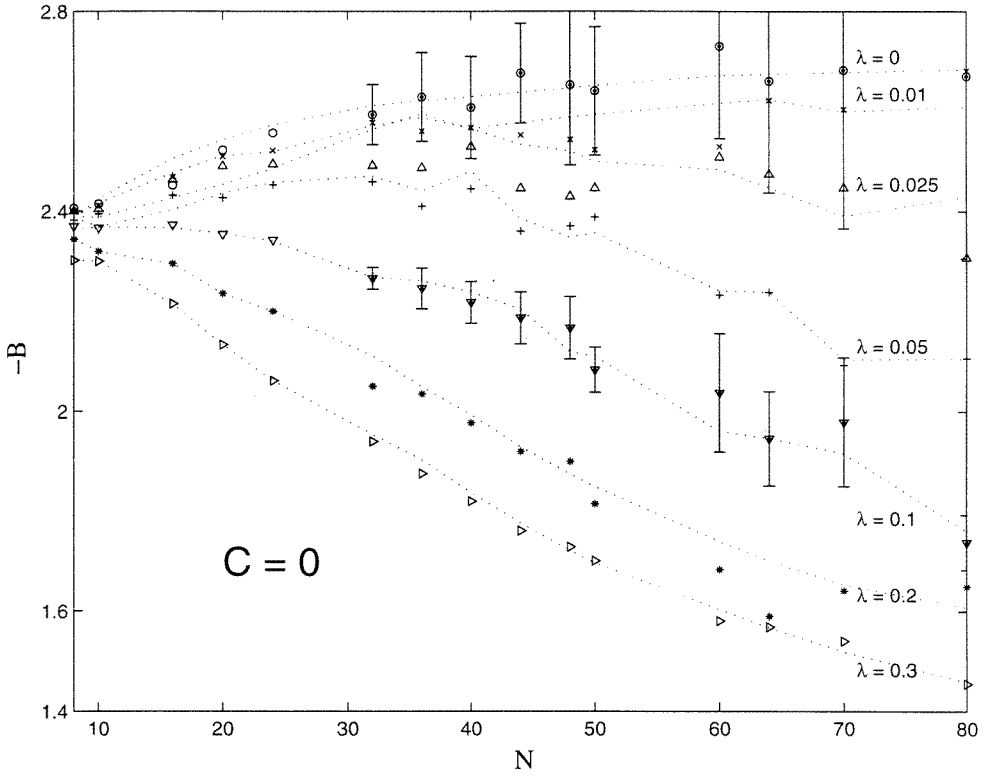

Figure 5. Values of $-B$ versus N for a polyelectrolyte chain at $\lambda = 0$ (SAW) and for various λ (Å) in the vicinity of $\lambda = 0$. The markers display the raw data. The dotted curves display the smoothed data (see section 4.4). Error bars for $\lambda = 0$ and for $\lambda = 0.1$ Å are shown for various N. Error bars are longer for higher N. As λ increases from zero, error bars are shorter as shown for $\lambda = 0.1$ Å.

an iterative smoothing algorithm that utilizes relations (5) and (6) between d_f, $-B$ and $\langle S^2 \rangle$. We start the process with the raw data from the simulation for d_f, $-B$ and $\langle S^2 \rangle$ and smooth these data iteratively. Each smoothing iteration consists of two steps. As the first step, we perform smoothing versus λ for each N using cubic spline approximation independently on each curve of d_f, $-B$ and $\langle S^2 \rangle$. The smoothed new values of $-B$ and d_f obtained at this step are then substituted in equations (5) and (6). For each λ, the percentage difference $\delta(\lambda)$ between the value of $\langle S^2 \rangle$ calculated from equation (5) and the value obtained from the smoothed simulation data at this step is recorded. For the λ values where $\delta(\lambda)_n < \delta(\lambda)_p$ (subscript n for new and p for previous), the values of d_f, $-B$, and $\langle S^2 \rangle$ are replaced with the new smoothed values. For λ values where $\delta(\lambda)_n > \delta(\lambda)_p$ we leave d_f, $-B$ and $\langle S^2 \rangle$ unchanged. In the second step of the iteration, we repeat this process at each λ for curves of d_f, $-B$ and $\langle S^2 \rangle$ versus N. For each N, the difference $\delta(N)$ between the value of $\langle S^2 \rangle$ calculated from equation (5) and the value obtained from the smoothing is recorded. For the N values where $\delta(N)_n < \delta(N)_p$, the values of d_f, $-B$ and $\langle S^2 \rangle$ are replaced with the new smoothed values. For N values where $\delta(N)_n > \delta(N)_p$ we leave d_f, $-B$ and $\langle S^2 \rangle$ unchanged. The two-step iteration described above is then repeated as needed until the maximum value of $\delta(\lambda)$ for all investigated λ in the first step and the maximum value of $\delta(N)$ for all investigated N in the second step are below 0.5 per cent.

For NSAW, the smoothing is necessary to discern clearly even the qualitative behaviour. For high λ, the qualitative behaviour is clear without smoothing. In [2], we use smoothing with respect to λ to improve the extrapolation results.

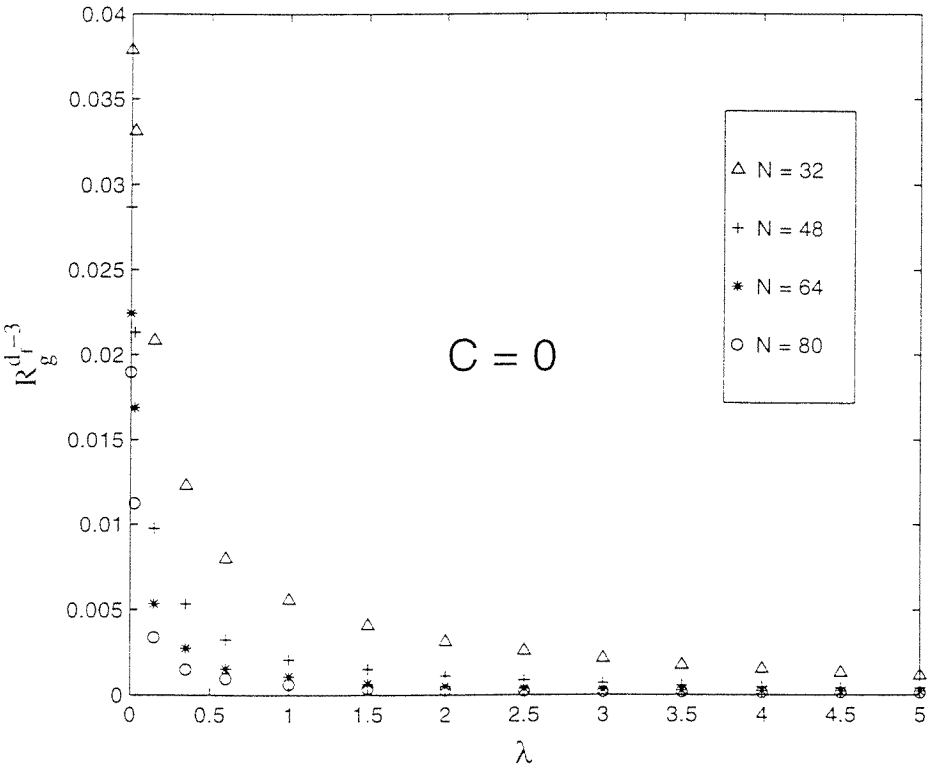

Figure 6. Values of $\langle S^2 \rangle^{(d_f-3)/2}$ versus λ (Å) for a bare polyelectrolyte chain ($C = 0$), with various number of beads, N.

4.5. Density of monomers at various λ

The density of N' polymer monomers in the volume within a sphere of radius of gyration $R_g = \langle S^2 \rangle^{1/2}$ is proportional to $N'/R_g^3 = R_g^{d_f-3}$ and is plotted versus λ in figure 6. Again, as for d_f, sharp decrease occurs in the range $0 < \lambda < 1$ Å. This may be evidence for the first-order nature of the phase transition envisaged by de Gennes for the coil-stretch transition of polymers under ultrahigh velocity gradients [53, 54]. De Gennes' 'afterthought' in [54] refers to [55] and references therein where experiments confirming this transition are described. For recent papers in this subject see [56, 57] and references therein. We do not expect to find discontinuities in the vicinity of $\lambda = 0$ in this first-order phase transition system because, as is known, it is impossible to find discontinuities in simulations of finite systems.

As λ increases, less contacts exist [12], therefore the probability of movement failure because of occupied sites is reduced. The suppression of the self-avoidance or excluded volume effects as the persistence length of the chain increases was discussed in [58] and references therein. Despite the suppression of the self-avoidance effects at high λ, the freedom of movement of the chain does not increase (except for λ less than approximately 0.3 Å, not shown). This is because the increase in the chain's rod-like character causes an increase in the global fraction of chain-move failures.

In figure 6 we do not observe large changes in the density in the vicinity of $\lambda \sim 8$ Å. This indicates that at $\lambda \sim 8$ Å, the phase transition [12, 36] might be a second-order transition.

5. Summary and concluding remarks

The most important merit of this paper is the first presentation, to the best of our knowledge, of a numerical method for evaluation of the fractal dimensionality, d_f over a continuous range of λ using techniques developed previously for random fractal objects. Drastically decreasing values of d_f, characteristic of a phase transition, are found as λ increases from zero in the range $0 < \lambda < 1$ Å. The fractal dimensionality approaches unity as predicted by de Gennes *et al* close to the onset of order (figure 2). The exponent behaviour is related to the mechanism of chain expansion.

In this study, we have found large changes in the values of d_f in the vicinity of $\lambda = 0$ both for systems of $C = 0$ and $C \neq 0$. This means that, in this regime of λ, there exists a strong sensitivity of the exponent to minor changes in physical condition as is typical of phase transitions. Systems of neutral expanding polymers and monolayers are expected to demonstrate similar behaviour. We have found that single polyelectrolyte chains of even very low counter-ion concentrations have $d_f > 1$ which means that their structure is not rod-like.

Owing to the sharp drop in d_f as λ rises above zero, we have inferred that the d_f values obtained from experimental measurements of neutral polymers with bulky side groups may be found smaller than the SAW results. Because of steric repulsion, bulky side groups on a backbone of even a neutral polymer raise λ to be effectively above zero. The sharp decrease of d_f in figure 2 indicates that experimental measurement of d_f of neutral polymer chain may yield results lower than the value expected for the SAW chain.

The sharp decrease in d_f as λ increases from zero may be caused by the sharp drop in contacts. The absence of contacts above $\lambda = 0$ may indicate that the polyelectrolyte problem is similar to the directed walks problem. Note, however, that the number of contacts is small relative to the number of kinks, which also decrease during the expansion. One would expect, therefore, that the decrease in both contacts and kinks is responsible for the sharp changes in d_f.

Another major finding in this paper is that, for $\lambda = 0$, there is no single d_f value for all investigated N. Rather than the previously-found constant value, the behaviour of d_f versus N at $\lambda = 0$ is shown to be non-monotonic. An increase with N has been found up to $N = 70$. Similar behaviour at low λ is found for the prefactor $-B$.

The noise in the d_f and $-B$ values at low λ (NSAW) obscures the behaviour with respect to N. Extensive investigation that involves smoothing of d_f, $-B$ and $\langle S^2 \rangle$ with respect to λ and to N simultaneously has yielded a substantial improvement in the MC results and has revealed the interesting fan-shaped behaviour of exponents at NSAW, i.e. at λ slightly above zero (figures 4 and 5). It also has enabled the discernment of a consistent trend, a non-monotonic behaviour of d_f and B versus N at $\lambda = 0$ and close to zero. To obtain more accurate data on both charged and uncharged chains, further investigation is required.

The exponents in the vicinity of $\lambda = 0$ were calculated again using numerical differentiation. From the results we see that the usual log–log method for exponent calculations, method I_a, yields exponents for a chain whose length is the *mean* of the investigated chain lengths rather than for an infinite chain as would be expected. For explanations see section 4.1.2.

The transition near $\lambda = 0$ from disorder to order can be considered as a kind of gas-to-liquid transition. The transition between two ordered phases near $\lambda = 8$ Å is reminiscent of the liquid-to-solid transition type. The phase transition at low λ seems to apply to both classes of phase transitions, thermal and structural. The phase transition in the vicinity of $\lambda = 8$ Å seems to be a geometric one. It is possible that the transition we find in this study for λ close to zero is connected to breaking-up of an SAW system symmetry.

Concerning the transition from thermal disorder to order it is interesting to note that Helgesen *et al* [59] showed that diffusing magnetized spheres in a plane produces aggregates

with fractal dimensionality d_f that decreases with increasing magnetic moment. Pastor-Satorras and Rubi [60] showed that diffusing clusters produces aggregates with d_f that decreases with increasing ratio of the magnetic dipole–dipole interactions to the temperature. In both these cases, similar to our study, d_f is found to decrease towards unity from its limiting value as the system becomes more ordered. We found a sharp transition in d_f which may be found also in these systems [59, 60] when larger clusters are investigated. In [60] different values for the fractal dimensionality were obtained for different values of N. This is similar to the different values of d_f that we find for polyelectrolytes at various N.

As an aside concerning self-similarity, we suggest a possible explanation for the power laws in the vicinity of the critical point. We believe that the dynamics of phase transitions are very similar to the dynamics of growth processes, during which self-similar structures described by power laws are created. The resemblance between phase transitions and growth processes near the critical point may be seen by the growth of spin clusters in Ising models, and the growth of the percolation clusters. The power laws reflect the fact that magnets or fluids are self-similar near their critical points. An historical introduction to the modern theory of critical phenomena is found in Cyril Domb's recent monograph [59].

The large size-effect observed in our previous papers for polyelectrolyte chains for $N \leqslant 32$ has been confirmed by this investigation. Short charged macrochains have been found to be bent more than long charged chains thereby adding a new explanation for the stability of the benzene structure.

Investigation of the parameter d_f for $0.01 \leqslant \lambda \leqslant 0.5$ Å (NSAW) has enhanced our understanding of exponent variation with N. Extension of the measurements to $\lambda < 0.01$ Å and to $N > 80$ can much improve our understanding of behaviour at $\lambda = 0$, the SAW chain model, which has proved to be a useful model of the dilute solution of linear polymers in good solvents.

Fractal dimensionality concepts have enabled the discovery of the phase transition in the vicinity of $\lambda = 0$ and its order. Using the d_f values we have plotted the polymer monomer density over a continuous range of λ for various N, and have obtained a sharp drop. Fractal investigations contributed to the development of the smoothing method that has enabled discernment of the fan-shaped behaviour in the vicinity of $\lambda = 0$.

Acknowledgments

CB thanks Penina (Shir) Sheinbaum and the Morris J and Betty Kaplun Foundation for their support. CB acknowledges the discussions with D Ben-Avraham, the questions and enlightening comments of David Bannett and the help of Ya'akov Sheinbaum with grateful thanks. CB appreciates the hospitality of the organizers of the 'Slow dynamical processes in heterogeneous soft matters' workshop and of the 19th IUPAP international conference on Statistical Physics during which parts of this paper were prepared.

References

[1] de Gennes P-G 1972 *Phys. Lett.* **38** 339
[2] Brender C, Danino M and Shatz S submitted
[3] Stevens M J and Kremer K 1995 *J. Chem. Phys.* **103** 1669
[4] Reed C and Reed W 1990 *J. Chem. Phys.* **92** 6916
[5] Ben-Avraham D 1982 Fractal dimensionality of polymers *MSc Thesis* Bar-Ilan University
[6] Havlin S and Ben-Avraham D 1982 *J. Phys. A: Math. Gen.* **15** L311
[7] Havlin S and Ben-Avraham D 1982 *J. Phys. A: Math. Gen.* **15** L317
[8] Havlin S and Ben-Avraham D 1982 *J. Phys. A: Math. Gen.* **15** L321

[9] Havlin S and Ben-Avraham D 1982 *Phys. Rev.* A **26** 1728
[10] Brender C, Ben-Avraham D and Havlin S 1983 *J. Stat. Phys.* **31** 661
[11] Brender C 1990 *J. Chem. Phys.* **92** 4468
[12] Brender C 1991 *J. Chem. Phys.* **94** 3213
[13] Brender C, Lax M and Windwer S 1981 *J. Chem. Phys.* **74** 2576
[14] Metropolis N, Rosenbluth A W, Rosenbluth M N, Teller A H and Teller E 1953 *J. Chem. Phys.* **21** 1087
[15] Kirkpatrick S, Gelatt C D Jr and Vecchi M P 1983 *Science* **220** 671
[16] Brender C and Danino M 1993 *Phys. Rev.* E **48** 3717
[17] de Gennes P-G 1985 *Scaling Concepts in Polymer Physics* 2nd edn (Ithaca, NY: Cornell University Press)
[18] Mandelbrot B B 1982 *The Fractal Geometry of Nature* (San Francisco, CA: Freeman)
[19] Bunde A and Havlin S 1994 *Fractals in Science* ed A Bunde and S Havlin (Berlin: Springer)
[20] Daoud M, Stanley H E and Stauffer D 1996 *Physical Properties of Polymers Handbook (AIP Series in Polymers and Complex Materials)* p 71
[21] Adler J 1983 *J. Phys. A: Math. Gen.* **16** L515
[22] Baumgärtner A 1984 *Application of the Monte Carlo Method in Statistical Physics* ed K Binder (Heidelberg: Springer)
[23] Rapaport D C 1985 *J. Phys. A: Math. Gen.* **18** 113
[24] Guttmann A J 1987 *J. Phys.* A **20** 1839
[25] Des Cloizeaux J and Jannink G 1990 *Polymers in Solution: Their Modelling and Structure* (New York: Oxford University Press)
[26] Dayantis J and Palierne J-F 1994 *Phys. Rev.* B **49** 3217
[27] Adam M and Lairez D 1993 *Fractals* **1** 149
[28] Sokal A D 1995 *Monte Carlo and Molecular Dynamics Simulations in Polymer Science* (New York: Oxford University Press) and references therein
[29] Everaers R, Graham I S and Zuckermann M J 1995 *J. Phys. A: Math. Gen.* **28** 1271
[30] Eizenberg N and Klafter J 1996 *Phys. Rev.* B **53** 5078
[31] Fisher M E 1998 *Rev. Mod. Phys.* **70** 653
[32] Aharony A 1998 *Science at the Turn of the Century, a Quintet of Symposia (Int. Conf. Jerusalem)*
[33] Domb C and Hioe F T 1969 *J. Chem. Phys.* **51** 1915
[34] Wall F T and Erpenbeck J J 1959 *J. Chem. Phys.* **30** 634
[35] Flory P J 1953 *Principles in Polymer Chemistry* (Ithaca, NY: Cornell University Press)
[36] Brender C 1992 *J. Phys. Chem.* **96** 5553
[37] de Gennes P-G, Pincus P, Velasco R M and Brochard F 1976 *J. Physique* **37** 1461
[38] Higgs P G and Orland H 1991 *J. Chem. Phys.* **95** 4506
[39] Brender C and Danino M 1992 *J. Chem. Phys.* **97** 2119
[40] Brender C and Danino M 1996 *J. Phys. Chem.* **100** 17563
[41] Majid I, Djordjevic Z and Stanley H E 1983 *Phys. Rev. Lett.* **51** 1282
[42] Shaik S 1996 *WATOC 96: 4th World Congress of Theoretically Oriented Chemists (Jerusalem)*
[43] Förster S and Schmidt M 1995 *Adv. Polym. Sci.* **120** 51
[44] Semenov A N, Duke T A J and Viovy J L 1995 *Phys. Rev.* E **51** 1520
[45] Goldman A 1996 *Int. Conf. on Condensed Matter Physics (Tel-Aviv)*
[46] Barr R, Brender C and Lax M 1980 *J. Chem. Phys.* **72** 2702
[47] Barr R, Brender C and Lax M 1981 *J. Chem. Phys.* **75** 453
[48] Bishop M and Clarke J H R 1990 *J. Chem. Phys.* **93** 1455
[49] Brender C 1990 *J. Chem. Phys.* **93** 2736
[50] Love J J, Li X, Case D A, Giese K, Grosschedl R and Wright P E 1995 *Nature* **376** 791
[51] Bruschweiler R, Liabo X and Wright P E 1995 *Science* **268** 886
[52] Brender C 1997 *Verbal Remark at the 62nd Meeting of the Israel Society 97 (Haifa)*
[53] de Gennes P-G 1974 *J. Chem. Phys.* **60** 5030
[54] de Gennes P-G 1992 *Simple Views on Condensed Matter* (Singapore: World Scientific)
[55] Keller A and Odell J 1985 *Colloid. Polym. Sci.* **263** 181
[56] de Gennes P-G 1997 *Science* **276** 1999
[57] Brochard-Wyart F and Buguin A 1997 *Mater. Res. Soc. Bull* **22** 48
[58] Privman V and Frisch H L 1988 *J. Chem. Phys.* **88** 469
[59] Helgesen G, Skjeltorp A T, Mors P M, Botet R and Jullien R 1988 *Phys. Rev. Lett.* **61** 1736
[60] Pastor-Satorras R and Rubi J M 1995 *Phys. Rev.* E **51** 5994
[61] Domb C 1996 *The Critical Point* (London: Taylor and Francis)